Journal of Solid State Chemistry **145,** 204–211 (1999)
Article ID jssc.1999.8243, available online at http://www.idealibrary.com on IDEAL®

Preparation, Electrical Properties, Crystal Structure, and Electronic Structure of Cu_4GeS_4

Xue-an Chen, Mitsuko Onoda, Hiroaki Wada,[1] Akira Sato, and Hiroshi Nozaki

National Institute for Research in Inorganic Materials, 1-1 Namiki, Tsukuba-shi, Ibaraki 305, Japan

and

Regine Herbst-Irmer

Institut für Anorganische Chemie, Universität Göttingen, Tammannstrasse 4, D-37077 Göttingen, Germany

Received August 17, 1998; in revised form February 12, 1999, accepted February 24, 1999

Cu_4GeS_4 was synthesized by the solid state reaction of the constituent binary chalcogenides at 830°C. Its crystal structure was determined on the basis of X-ray data of a nonmerohedral twinned crystal: monoclinic $P2_1/c$, $a = 9.790(2)$, $b = 13.205(2)$, $c = 9.942(3)$ Å, $\beta = 100.90(2)^\circ$, $Z = 8$. The refinement of 164 parameters with 1373 data converged to $R_1 = 0.058$ [for $I > 2\sigma(I)$], w$R_2 = 0.176$ (all data), and a twin fraction of 0.274(4). The crystal structure may be described as a monoclinic variant of the Cu_4SnS_4 type. It is characterized by a three-dimensional framework based on a hexagonal close-packing of sulfur atoms. The Cu and Ge atoms are distributed in an ordered manner over 5/8 of the tetrahedral voids, with half of the Cu atoms distorted into triangular sites. The structure was compared with that of Cu_4SnS_4, and the difference was ascribed to the formation of more triangular Cu sites in Cu_4GeS_4. An extended Hückel tight-binding band calculation was performed to analyze the electronic structure, and electrical resistivity measurements confirm the expected semiconducting behavior of Cu_4GeS_4.

INTRODUCTION

The Ag- and Cu-containing chalcogenides have attracted much attention due to their unusual structural features, e.g., forming 1-D, 2-D, and 3-D solids, and their interesting physical properties including ionic conductivity. The interest in these materials has led to our recent discovery of two new structure types of $Cu_4Sn_7S_{16}$ and Cu_4SnS_6 (1, 2). Although the elements Ge and Sn have similar electronic configurations and chemical behaviors, the compounds formed in the Cu–Ge–S system are slightly different from those in the Sn-containing system. For example, the argyrodite-type Cu_8GeS_6 phase does not appear in the Cu–Sn–S system. Conversely, for the spinel-like $Cu_4Sn_7S_{16}$, no corresponding Ge-analogue could be obtained in our experiments. The phase diagram of the ternary system copper–germanium–sulfur has been investigated by Wang (3), who proposed a lot of new phases, and most of them are stable within a narrow temperature region below 500°C. Above this temperature, three ternary phases were confirmed, of which Cu_2GeS_3 was recently characterized by single crystal X-ray diffraction techniques (4). It is a sphalerite superstructure based on a cubic close-packed array of sulfur atoms with space group Cc. Cu_8GeS_6 was reported to be dimorphic with a phase transition at 57(2)°C (5), the high-temperature phase of which was not quenchable and isotypic with the cubic Ag_8GeTe_6 structure (6), and the low-temperature phase crystallized in an orthorhombic β-Cu_8SiS_6 type (7). Cu_4GeS_4 was reported to be stable at a temperature above 605°C. Based on the precession photographs, this compound was predicted to be orthorhombic with possible space group $A2_122$ (8). However, its crystal structure remains as yet undetermined. Our present X-ray structure analysis found the space group of this compound actually to be monoclinic $P2_1/c$. In addition, we also report its band electronic structure and electrical behavior.

SAMPLE PREPARATION AND CHARACTERIZATION

The compound Cu_4GeS_4 was synthesized by a stoichiometric mixture of Cu_2S (1.061g, 6.67 mmol; Rare Metallic, 99.9%) and GeS_2 (0.456g, 3.33 mmol; Rare Metallic, 99.9%). The sample was ground in an agate mortar and pressed into pellets. The pellets were introduced into a silica tube and sealed at a pressure of less than 10^{-3} Torr. The tubes were held at 700°C for one week, then heated gradually to 830°C,

[1]To whom correspondence should be addressed. Fax: 81-298-52-7449; E-mail: wadah@nirim.go.jp.

0022-4596/99 $30.00

where they were kept for one month, and then cooled at a rate of 5°C/h to 690°C and quenched in cold water. The gray crystals with metallic luster were found in the tubes, and they had the shape of prisms with dimensions up to $0.4 \times 0.4 \times 0.8$ mm^3. The compound appears to be relatively stable in air and water. The chemical composition of the crystals was determined by means of a JEOL JXA-8600 MX electron microprobe, using $Bi_4Ge_3O_{12}$ and $CuFeS_2$ as standards for Ge, Cu, and S, respectively. An approximate atomic ratio Cu:Ge:S of 4.1:1.0:4.2 was obtained, which is in good agreement with that deduced from the structural refinement. In addition, a small amount of triangular platelike crystals was also observed in the reaction product. X-ray four-circle diffractometer data indicated that the reciprocal lattice of these crystals mimicked trigonal symmetry $-3m$ with a pseudohexagonal cell $a_h = 13.986$ and $c_h = 17.058$ Å. They turned out to be the rhombohedral twinning of the Cu_8GeS_6 phase (9).

For the accurate lattice constant determination, X-ray powder diffraction data were collected by using the monochromatized Cu$K\alpha$1 radiation of a Rigaku RINT 2000 diffractometer. The powder XRD data for the structure refinement were recorded in $2\theta = 10°$–$100°$ with a step size of 0.02° and a counting time of 15 s.

An electrical resistivity measurement of copper germanium sulfide was made from liquid N_2 temperature to 300 K by a conventional dc four-probe method. A cold pressed pellet of sample Cu_4GeS_4 was cut suitably and polished into a rectangular form with the dimension of $2.55 \times 1.70 \times 2.30$ mm^3. Electrical contacts were made using silver paste.

Electronic structure calculations were carried out by means of the extended Hückel method within the framework of the tight-binding approximation (10–11). Atomic parameters for the elements were taken from the literatures (12–13) and they are listed in Table 1. The off-diagonal matrix elements of the Hamiltonian were evaluated by means of a weighted formula (14). A set of 80 k-points in the irreducible part of the Brillouin zone was used for the average properties calculations (15).

TABLE 1
Extended Hückel Parameters

Atom	Orbital	H_{ii} (eV)	ξ_1	ξ_2	c_1	c_2
S	3s	−20.00	2.122			
	3p	−13.30	1.827			
Cu	4s	−11.40	2.200			
	4p	−6.06	2.200			
	3d	−14.00	5.950	2.30	0.5933	0.5744
Ge	4s	−16.00	2.160			
	4p	−9.00	1.850			

Note. H_{ii}, diagonal matrix elements of the EH Hamiltonian; ξ_i, the Slater exponents; c_i, the expansion coefficients.

STRUCTURE DETERMINATIONS

Cu_4GeS_4 has a pseudo-orthorhombic symmetry, and the crystals have a strong tendency to be twinning. Of the eight crystals examined in a Buerger precession camera, all exhibited apparent *mmm* Laue symmetry. Some reflection spots are very strong and sharp, while some others are split. An attempt to find an untwinned crystal failed. The cell dimensions obtained from the precession photographs ($a = 12.565$, $b = 15.215$, and $c = 13.205$ Å) were very similar to those reported by Wang (8). However, the structure could not be solved in any of the possible orthorhombic groups. A structure solution was finally found in the monoclinic centrosymmetric $P2_1/c$ group based on the lattice constants $a = 9.790(2)$, $b = 13.205(2)$, $c = 9.942(3)$ Å, and $\beta = 100.90(2)°$. This monoclinic primitive unit cell can be transformed to the above orthorhombic C-centered setting by a matrix $(-1\,0\,-1\;1\,0\,-1\;0\,-1\,0)$. The twin may be interpreted either as a rotation twin with twin axis $[10\bar{1}]$ or $[101]$ or as a reflection twin with twin plane $(10\bar{1})$ or (101), as that observed in arsenopyrite (16). One twin domain is related to the other by the interchange of the a and c axes. Because a and c differ by a factor of about 0.985 instead of 1, the overlap of the two reciprocal lattices is not quite exact. It can therefore be classified as a nonmerohedral twin and twin individuals have a volume ratio of about 1:3 for the crystal used for the structure determination. Examination of the intensity data indicated that a small amount of reflections $h0l$ with $h = 2n$ and $l = 2n + 1$ violate the systematic absences of the $P2_1/c$ group, confirming the twin model.

In order to confirm the monoclinic symmetry, X-ray powder diffraction data were recorded using Cu$K\alpha$1 radiation ($\lambda = 1.54051$ Å). The refined lattice constants ($a = 9.790(2)$, $b = 13.205(2)$, $c = 9.942(3)$ Å, and $\beta = 100.90(2)°$) are in good agreement with those obtained from the four-circle diffractometer data (Table 2). The structure was further refined from powder data (Fig. 1) using the Rietveld method with the program PREMOS (17). Two peaks at about $2\theta = 28.82°$ and 59.50° were removed, because they probably represent some small amount of unknown impurity phases which are unstable in air (when the sample was first scanned in a continuous mode, these two peaks were relatively weak. About 30 h later, the same sample together with the etched-glass holder was used for the step-scan—they became very sharp.). The initial positional parameters were taken from the single crystal method. In total, 75 parameters, including structural, polynomial background, and other global parameters, were simultaneously refined, and the pseudo-Voigt function was used to simulate the individual XRD peak profile. The refinement quickly converged to $Rwp = 5.67\%$, supporting the proposed structural model.

Intensity data were collected on an Enraf-Nonius CAD4 automatic four-circle diffractometer with graphite

TABLE 2
Some Data and Results of the Structure Determination of Cu_4GeS_4

Chemical formula	Cu_4GeS_4
Formula weight	454.99
Crystal dimension (mm)	$0.22 \times 0.20 \times 0.18$
Space group	$P2_1/c$ (No. 14)
Lattice constants	
From powder data	
a (Å)	9.790(2)
b (Å)	13.205(2)
c (Å)	9.942(3)
β (°)	100.90(2)
Volume (Å^3)	1262.1(5)
From single-crystal data	
a (Å)	9.797(2)
b (Å)	13.199(2)
c (Å)	9.921(3)
β (°)	100.90(2)
Volume (Å^3)	1259.7(5)
Z	8
Calculated density (g cm^{-3})	4.789
Temperature of data collection (K)	293
Wavelength (λMo$K\alpha$) (Å)	0.71073
Linear absorption coefficient μ (cm^{-1})	191.61
Transmission factors	0.0197–0.1397
ω–2θ scans up to	60°
Range in hkl	0–13, 0–18, $\pm$13
Total number of reflections	8020
Unique reflections refined	1373
Inner residual	$R_i = 0.041$
Reflections with $I > 2\sigma(I)$	750
Number of variables	164
BASF (refined twin fraction)	0.274(4)
S (Goodness-of-fit on F^2)	0.986
Weighting scheme	$w = 1/[\sigma^2(F^2) + (0.0919P)^2]$ here $P = (F_o^2 + 2F_c^2)/3$
R_1 [$I > 2\sigma(I)$]	0.058
wR_2 (all data)	0.176
$(\Delta/\sigma)_{max}$	0.000
Largest diff. peak and hole (e Å^{-3})	1.66, $-$1.27

monochromated Mo$K\alpha$ radiation. Cell dimensions for the single-crystal method were obtained from a least-squares refinement with 25 automatically centered reflections in the range $30° < 2\theta < 50°$. Three standard reflections were remeasured after every 200 reflections with no indication of crystal decay. The intensity data were corrected for Lorentz and polarization effects and for absorption by a Gaussian numerical integration using the measured dimensions of the crystal (18). The crystallographic data and some results are summarized in Table 2.

The structure was solved by direct methods in the SIR-92 program (19) and refined in SHELXL-97 system (20) by full-matrix least-squares methods on F_o^2. In an earlier work (8), the homogeneous Cu_4GeS_4 material was synthesized from a starting composition of 69 wt.% Cu_2S and 31 wt.% GeS_2, corresponding to the atomic ratio Cu:Ge:S = 3.91:1.02:4.00. In our present structure refinement, in order to check for deviations from the ideal compositions, occupancy parameters of Cu and Ge atoms were allowed to vary along with the positional and thermal parameters, while the occupancy parameters of S atoms were fixed at 1.0. The resulting occupancies varied between the values of 0.98(2) for Cu3 and 1.00(2) for Ge2. They are all within one standard deviation of the ideal values. Therefore, in the final least-squares cycles, the ideal occupancies were assumed. After averaging equivalent reflections, 3648 unique reflections were obtained, of which 2001 were observed with $I > 2\sigma(I)$. In a first refinement the reciprocal lattices of the two domains were assumed to be exactly superimposed and all of the unique reflections were included in the LS cycles taking the twinning into account (21–22). The R_1 converged to 0.074 for 2001 observed reflections, the residual electron densities ranged from -2.80 to 3.28 e Å^{-3}, and the refined twin ratio was 0.219(3). But only some reflections overlap nearly exactly, while a few are not affected by the twinning and others overlap only partially. Some partially overlapping reflections have been omitted, because the partial overlap makes it difficult to determine the background accuracy and the contribution of each domain. Assuming a contribution of both domains only for the nearly exact overlapping reflections the refinement of 164 parameters with 1373 data resulted in the residuals of $R_1 = 0.058$ (for $I > 2\sigma(I)$), $wR_2 = 0.176$ (all data), and a twin ratio of 0.274(4). A final difference Fourier map showed maximum and minimum electron densities of 1.66 and -1.27 e Å^{-3} at positions which are very close to the Cu1 and Ge2 sites (0.79 and 1.59 Å), respectively. Still some partially overlapping reflections are treated as exactly overlapping resulting in relatively high R values and residual electron density, but omitting all of them would reduce the number of data too much. The program MISSYM (23) did not reveal potential additional symmetry. The final positional, the equivalent isotropic and anisotropic displacement parameters, are given in Table 3. Listings of the structure factors are available from the authors.

DISCUSSION

Cu_4GeS_4 represents a new structure type (Pearson symbol $mP72$), and its crystal structure is characterized by a three-dimensional framework of CuS_4 and GeS_4 tetrahedra and CuS_3 triangles (Fig. 2). Each GeS_4 tetrahedron shares its four vertices with different CuS_4 tetrahedra and CuS_3 triangles, and the copper-centered tetrahedra and triangles are interconnected to each other by both corner- and edge-sharing. Figure 3 shows one h.c.p. AB sulfur stacking sheet with the filled cations. Four similar sheets are joined together to form one translation period of the monoclinic [101] direction. As can be seen, the sulfur atoms form

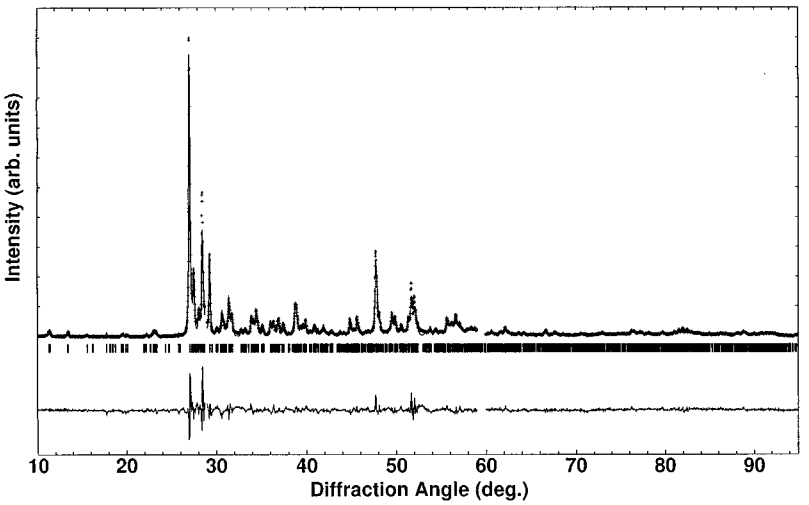

FIG. 1. Observed (+) and calculated (−) profiles for the Rietveld refinement of Cu_4GeS_4. A difference curve is plotted at the bottom. The vertical bars indicate the reflection positions.

a slightly distorted hexagonal close-packed arrangement, and the Cu and Ge atoms are distributed in an ordered manner over the tetrahedral voids between the S-layers, while the octahedral voids remain vacant. Of the available tetrahedral sites, one half are filled with Cu atoms, and one eighth with Ge atoms. Half of the Cu atoms are displaced from the tetrahedral centers toward one of the triangular faces, forming the triangular sulfur coordinations. Because more than 50% of the tetrahedral voids are filled by cations, numerous relatively short Cu–Cu contacts were obseved (Fig. 2). For example, Cu–Cu distances ranging from 2.548(7) to 3.071(6) Å were found not only between two edge-sharing CuS_4 tetrahedra (Cu5...Cu7, Cu5…Cu8), and between the edge-sharing CuS_3 triangles and CuS_4 tetrahedra (Cu3…Cu8), but also between two corner-sharing CuS_3 triangles (Cu1…Cu2). Some of them, like Cu2…Cu2^g

TABLE 3
Atomic Coordinates, Equivalent Isotropic and Anisotropic Displacement Parameters (Å^2) for Cu_4GeS_4

Atom	x	y	z	Ueq	U_{11}	U_{22}	U_{33}	U_{23}	U_{13}	U_{12}
Ge1	0.0578(3)	0.4118(2)	0.3110(3)	0.012(1)	0.012(2)	0.012(1)	0.012(1)	0.000(1)	0.004(1)	0.003(1)
Ge2	0.5496(3)	0.0909(2)	0.3025(3)	0.011(1)	0.013(2)	0.013(1)	0.007(1)	0.000(1)	0.002(1)	0.000(1)
Cu1	0.0840(4)	0.6900(3)	0.0142(5)	0.036(1)	0.022(3)	0.042(2)	0.037(3)	−0.014(2)	−0.009(3)	0.001(2)
Cu2	0.1283(5)	0.0483(2)	0.4763(5)	0.035(1)	0.039(3)	0.034(2)	0.026(2)	−0.010(2)	−0.011(2)	0.016(2)
Cu3	0.1628(5)	0.6809(3)	0.2855(5)	0.036(1)	0.023(3)	0.038(2)	0.045(3)	−0.005(2)	0.000(3)	−0.008(2)
Cu4	0.1850(4)	0.1539(2)	0.1799(4)	0.026(1)	0.026(2)	0.034(2)	0.020(2)	−0.009(2)	0.005(2)	−0.002(2)
Cu5	0.2884(5)	0.5801(3)	0.5298(5)	0.051(2)	0.082(5)	0.033(2)	0.044(3)	−0.012(2)	0.033(3)	−0.021(2)
Cu6	0.3525(5)	0.3612(3)	0.0831(5)	0.045(1)	0.051(4)	0.049(2)	0.033(3)	−0.018(2)	0.005(2)	−0.005(2)
Cu7	0.4194(4)	0.3369(2)	0.4275(5)	0.031(1)	0.022(2)	0.031(2)	0.039(3)	−0.007(2)	0.006(2)	0.003(2)
Cu8	0.6746(5)	0.3478(2)	0.1719(4)	0.031(1)	0.037(3)	0.034(2)	0.023(2)	0.008(2)	0.009(2)	0.005(2)
S1	0.0091(8)	0.0672(4)	0.2579(7)	0.015(2)	0.014(4)	0.014(2)	0.019(4)	−0.001(2)	0.006(3)	0.003(3)
S2	0.1204(7)	0.3273(4)	0.1348(6)	0.013(1)	0.013(4)	0.015(2)	0.012(3)	−0.004(2)	0.002(3)	0.000(3)
S3	0.1285(7)	0.8319(4)	0.1423(6)	0.014(1)	0.010(3)	0.019(2)	0.014(3)	−0.006(2)	0.007(3)	0.005(3)
S4	0.2350(7)	0.4152(4)	0.4888(7)	0.017(2)	0.021(4)	0.020(2)	0.012(3)	−0.003(2)	0.007(3)	−0.004(3)
S5	0.2696(7)	0.5875(4)	0.0191(7)	0.016(2)	0.014(4)	0.022(2)	0.012(3)	0.000(3)	0.000(3)	−0.001(3)
S6	0.3746(7)	0.1713(4)	0.3638(7)	0.017(2)	0.014(4)	0.018(2)	0.019(4)	0.001(3)	0.004(3)	0.001(3)
S7	0.5045(8)	0.4314(4)	0.2590(6)	0.014(1)	0.018(4)	0.014(2)	0.008(3)	−0.002(2)	0.000(3)	0.002(3)
S8	0.6060(8)	0.1745(4)	0.1245(6)	0.017(2)	0.022(4)	0.018(2)	0.011(3)	0.005(3)	0.000(4)	−0.008(3)

Notes. U_{eq} is defined as one third of the trace of the orthogonalized U_{ij} tensor. The anisotropic displacement factor exponent takes the form: $-2\pi^2(h^2a^{*2}U_{11} + \cdots + 2hka^*b^*U_{12})$.

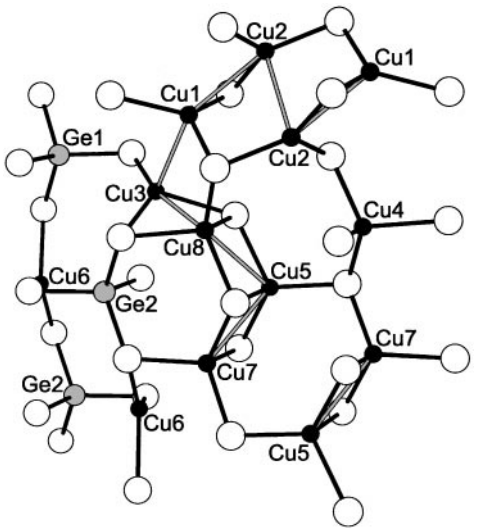

FIG. 2. Portion of the structure of Cu_4GeS_4 to show atomic coordinations. Large open circles, S; medium gray circles, Ge; small black circles, Cu atoms. Both Ge–S and Cu–S bonds are drawn with solid lines, while the Cu…Cu interactions less than 3.08 Å are represented by gray lines. Only cations are labeled for clarity.

of 2.934(9) Å and Cu1…Cu3^e of 3.055(6) Å (Table 4), are between two copper atoms which are located on two opposite triangular faces of a S_6 octahedron. These distances can be compared to the Cu–Cu bond distance of 2.56 Å observed in elemental Cu, and it is not surprising because similar short Cu–Cu separations were previously observed in low temperature chalcocite (2.52 Å upward) and djurleite (2.45 Å upward) (24), in ternary or quaternary chalcogenides like $Na_2Cu_4S_3$ (2.581(1) Å upward), KCu_3Te_2 (2.494(6) Å upward) (25), and $K_{1.5}Dy_2Cu_{2.5}Te_5$ (2.561(2) Å) (26). More compounds with short Cu…Cu distances

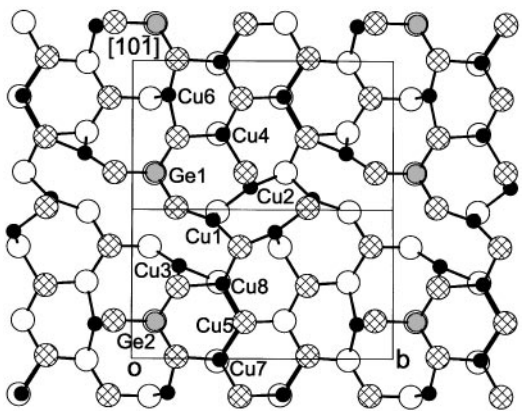

FIG. 3. Projection along the monoclinic [−10−1] direction of one *AB* sulfur stacking sheet, with the inserted cations. Large open circles are S atoms in *A* layer, large cross-hatched circles are S atoms in *B* layer of the *hcp* lattice, medium gray circles are Ge atoms, and small black circles are Cu atoms.

TABLE 4
Selected Bond Lengths (Å) and Angle (°) for Cu_4GeS_4

Ge1–S1^a	2.222(6)	Cu5–S3^i	2.391(7)
Ge1–S3^b	2.231(6)	Cu5–S7^k	2.634(8)
Ge1–S4	2.231(8)	Cu6–S7	2.269(8)
Ge1–S2	2.258(6)	Cu6–S6^j	2.272(8)
Ge2–S6	2.197(7)	Cu6–S2	2.464(8)
Ge2–S7^c	2.229(6)	Cu7–S4	2.261(8)
Ge2–S8	2.242(6)	Cu7–S6	2.296(7)
Ge2–S5^c	2.257(8)	Cu7–S7	2.364(7)
Cu1–S5	2.259(7)	Cu7–S8^f	2.417(8)
Cu1–S3	2.262(7)	Cu8–S5^l	2.242(7)
Cu1–S2^d	2.265(8)	Cu8–S7	2.299(7)
Cu2–S5^f	2.256(7)	Cu8–S8	2.406(7)
Cu2–S1	2.277(9)	Cu8–S3^c	2.413(8)
Cu2–S2^f	2.288(7)	Cu1–Cu3	2.665(7)
Cu3–S1^a	2.236(7)	Cu1–Cu2^a	2.812(6)
Cu3–S8^h	2.273(9)	Cu1–Cu3^e	3.055(6)
Cu3–S3	2.436(7)	Cu2–Cu6^f	2.548(7)
Cu4–S4^j	2.245(7)	Cu2–Cu2^g	2.934(9)
Cu4–S1	2.320(7)	Cu3–Cu8^h	2.704(5)
Cu4–S6	2.357(8)	Cu3–Cu5	2.838(7)
Cu4–S2	2.394(6)	Cu5–Cu7^k	3.018(7)
Cu5–S4	2.258(7)	Cu5–Cu8^k	3.071(6)
Cu5–S8^h	2.362(8)		
S1^a–Ge1–S3^b	107.2(3)	S4^j–Cu4–S2	108.8(3)
S1^a–Ge1–S4	111.4(3)	S1–Cu4–S2	110.4(3)
S3^b–Ge1–S4	112.9(3)	S6–Cu4–S2	101.2(3)
S1^a–Ge1–S2	109.0(2)	S4–Cu5–S8^h	120.4(3)
S3^b–Ge1–S2	106.3(2)	S4–Cu5–S3^i	113.8(3)
S4–Ge1–S2	109.9(3)	S8^h–Cu5–S3^i	117.0(3)
S6–Ge2–S7^c	112.1(3)	S4–Cu5–S7^k	101.9(3)
S6–Ge2–S8	107.6(3)	S8^h–Cu5–S7^k	100.5(3)
S7^c–Ge2–S8	109.3(2)	S3^i–Cu5–S7^k	97.4(3)
S6–Ge2–S5^c	109.2(3)	S7–Cu6–S6^j	130.5(3)
S7^c–Ge2–S5^c	107.9(3)	S7–Cu6–S2	114.2(3)
S8–Ge2–S5^c	110.9(3)	S6^j–Cu6–S2	115.1(3)
S5–Cu1–S3	114.6(3)	S4–Cu7–S6	112.9(3)
S5–Cu1–S2^d	124.2(3)	S4–Cu7–S7	110.8(2)
S3–Cu1–S2^d	120.2(3)	S6–Cu7–S7	112.4(3)
S5^f–Cu2–S1	116.9(3)	S4–Cu7–S8^f	109.3(3)
S5^f–Cu2–S2^f	122.7(3)	S6–Cu7–S8^f	103.9(3)
S1–Cu2–S2^f	120.0(3)	S7–Cu7–S8^f	107.1(3)
S1^a–Cu3–S8^h	135.1(3)	S5^l–Cu8–S7	116.5(3)
S1^a–Cu3–S3	114.9(3)	S5^l–Cu8–S8	107.5(3)
S8^h–Cu3–S3	106.1(3)	S7–Cu8–S8	109.6(3)
S4^j–Cu4–S1	112.1(3)	S5^l–Cu8–S3^c	113.2(3)
S4^j–Cu4–S6	115.5(3)	S7–Cu8–S3^c	106.5(3)
S1–Cu4–S6	108.3(3)	S8–Cu8–S3^c	102.7(3)

Note. The lattice constants obtained from powder data were used to calculate the interatomic distances. Symmetry codes: $^a -x,\ y+1/2,\ -z+1/2$; $^b -x,\ y-1/2,\ -z+1/2$; $^c -x+1,\ y-1/2,\ -z+1/2$; $^d -x,\ -y+1,\ -z$; $^e x,\ -y+3/2,\ z-1/2$; $^f x,\ -y+1/2,\ z+1/2$; $^g -x,\ -y,\ -z+1$; $^h -x+1,\ y+1/2,\ -z+1/2$; $^i x,\ -y+3/2,\ z+1/2$; $^j x,\ -y+1/2,\ z-1/2$; $^k -x+1,\ -y+1,\ -z+1$; $^l -x+1,\ -y+1,\ -z$.

(d^{10}–d^{10} interactions) have been recently reviewed (27). The copper distribution forms a zigzag chain (Fig. 2), suggesting that the title compound may be an ionic conductor at high temperature.

Table 4 lists the selected bond distances and angles concerning the coordination geometries of the cation-centered sulfur polyhedra. The tetrahedral environments around two germanium atoms are almost regular, with the S–Ge–S angles being near the tetrahedral value. The Ge–S bond lengths lie within a narrow range of 2.197(7) to 2.258(6) Å, which are in good agreement with those found in compounds such as Cu_2GeS_3 (2.185(5)–2.328(4) Å) (4), and $KLaGeS_4$ (2.203(1)–2.220(1) Å) (28). There are eight crystallographically distinct copper atoms, of which Cu1, Cu2, Cu3, and Cu6 are in triangular coordination and Cu4, Cu5, Cu7, and Cu8 are in tetrahedral coordination. Both coordination configurations are distorted. The Cu–S bonds in the tetrahedra range from 2.242(7) to 2.634(8) Å, and the S–Cu–S angles from 97.4(3)° to 120.4(3)°; in the triangles the respective ranges are 2.236(7) to 2.464(8) Å and 106.1(3)° to 135.1(3)°. Depending on the considered sites, the mean values of the Cu–S distances extend from 2.329(8) to 2.411(8) Å for the tetrahedral and 2.262(8) to 2.335(8) Å for the triangular sites, respectively. They are closely comparable to those found in the literature. For example, the average Cu–S bond lengths are 2.333(1) and 2.342(2) Å in Cu_4TiS_4 where both of the copper sites are four-coodinated (29), and for the triangular copper atom the mean value of 2.33(1) Å was observed in $TlCu_3S_2$ (30) and 2.1915(4) Å in covellite CuS (31). The longest average Cu–S distance is on the Cu5 site (2.411(8) Å). This is understandable because each Cu5-centered tetrahedron shares two edges with Cu7- and Cu8-centered tetrahedra (Fig. 2), forming three elongated and one shortened Cu–S bonds.

In this structure, two Ge and eight S positions are well defined, as revealed by their smaller and comparable equivalent thermal factors U_{eq} (Table 3), while the Cu atoms show abnormally high atomic displacement parameters. This is a specific characteristic of the d^{10} cations and has been observed in many other Ag^+- and Cu^+-containing chalcogenides like $CuVP_2S_6$ (32) and $AgScP_2S_6$ (33). It was explained as resulting from a static disorder generated by several off-center displacements of the cations (34), and these displacements were attributed to a second-order Jahn–Teller effect involving the filled d orbitals (35).

The crystal structure of Cu_4GeS_4 is closely related to that of Cu_4SnS_4 (36), and it may be described as a monoclinic variant of the Cu_4SnS_4 type. The space group $P2_1/c$ of Cu_4GeS_4 is a maximal nonisomorphic subgroup (index 2) of the group *Pnma* adopted by Cu_4SnS_4. The symmetry reduction represents a step which is "*translationengleich*." The lattice vectors of Cu_4GeS_4 (**a**, **b**, and **c**) are related to those of Cu_4SnS_4 ($\mathbf{a}_1$, $\mathbf{a}_2$, and $\mathbf{a}_3$) in the following manner: $\mathbf{a} = \mathbf{a}_2 - \mathbf{a}_3$, $\mathbf{b} = \mathbf{a}_1$, and $\mathbf{c} = -\mathbf{a}_2 - \mathbf{a}_3$. Figure 4 shows the projection of Cu_4GeS_4 structure along the monoclinic $[-10-1]$ vector together with the c-axis projection of the Cu_4SnS_4 structure. For simplicity, only half a translation period of the monoclinic $[10-1]$ vector was displayed, and

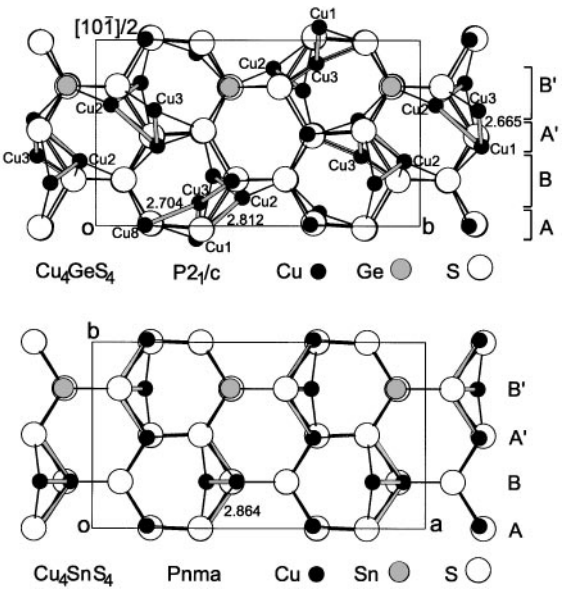

FIG. 4. The crystal structure of Cu_4GeS_4 projected along the monoclinic $[-10-1]$ vector as compared to the orthorhombic (*Pnma*) structure of Cu_4SnS_4. Ge–S (Sn–S) and Cu–S bonds are drawn with thin solid lines, while the Cu…Cu contacts less than 2.9 Å are represented by thick gray lines. The layers A, B, A', and B' in Cu_4SnS_4 correspond to $y = 0$, 0.25, 0.5 and 0.75, respectively, and the similar layers in Cu_4GeS_4 which correspond to those in Cu_4SnS_4 are also marked.

the other half of the structure is similar and can be obtained from this arrangement by a translation [**101**]/2 together with [**10−1**]/2. It can be seen that the germanium- and copper-centered sulfur polyhedra form distorted hexagonal windows running along this projection direction, and the centers of these windows correspond to the unoccupied octahedral sites. Although copper atoms were often found to be statistically distributed over several positions (32), our difference Fourier analyses did not reveal any significant electron-density peak within these pseudohexagonal channels. Both structures were arbitrarily divided into atomic layers for comparison. It was observed that the layers B and B' in Cu_4SnS_4 are situated on the mirror plane of the orthorhombic (*Pnma*) structure and therefore they are completely flat, while the corresponding layers in Cu_4GeS_4 are strongly puckered with an amplitude of about ± 0.968 Å. Similarly, the layers designated A and A' in Cu_4SnS_4 are slightly distorted ($\Delta y = \pm 0.095$ Å), whereas the corresponding layers in Cu_4GeS_4 are apparently more distorted, with atomic displacements out of the plane by about ± 0.531 Å. A comparison of the atomic parameters demonstrates that the Ge and S positions in Cu_4GeS_4 remain close to those of Sn and S atoms in Cu_4SnS_4, while some of the Cu sites show much greater distortions. For instance, Cu2 and Cu3 atoms at the layers B and B' of Cu_4GeS_4 shift toward their neighboring atomic layers (A and A') to form relatively short Cu–Cu contacts. The observed interlayer

Cu1–Cu2, Cu1–Cu3, and Cu3–Cu8 distances are 2.812(6), 2.665(7), and 2.704(5) Å, respectively, significantly shorter than the corresponding ones in Cu_4SnS_4 (2.864 Å). It is noteworthy that one half of Cu atoms in Cu_4GeS_4 have trigonal sulfur environments, while only one quarter of Cu atoms in Cu_4SnS_4 have such coordinations. The displacements of the tetrahedral Cu atoms out of the mirror plane result in the formation of more triangular Cu sites, which in turn causes a lowering of the space-group symmetry in going from Cu_4SnS_4 to Cu_4GeS_4. The fact that Cu(I) favors the lower coordination number was explained as a second-order Jahn–Teller coupling between the occupied 3*d* and the empty 4*s* orbitals (35).

The shortest S...S contact in Cu_4GeS_4 is 3.582(9) Å, which is close to the van der Waals radii sum of 3.60 Å (37) and significantly longer than 2.07 Å, expected for S–S single bonds (38). The lack of close S–S interactions as well as the semiconducting behavior is consistent with the closed-shell description $Cu_4^{1+}Ge^{4+}S_4^{2-}$. This structural model was further checked by the bond valence sum (BVS) analysis using Brown's formula (39, 40). The resulting BVS values range from 3.84 to 3.89 for Ge, 0.86 to 1.13 for Cu, and −1.94 to −2.00 for S, respectively, consistent with their assigned formal valences.

Tight-binding band structure calculations were performed on the three-dimensional Cu_4GeS_4 material of the complete structure. The diagrams of the total and projected density of states (DOS) were displayed in Fig. 5. Inspection of the projected DOS curves shows that the upper valence band is primarily composed of Cu 3*d* and S 3*p* orbitals, with the S 3*p* penetrating into the Cu 3*d* states, indicating the strong Cu–S covalent hybridizations, whereas the conduction band has mainly Cu 4*s* and 4*p* as well as Ge 4*s* and 4*p* character, and the latter is still higher in energy. The bands in the energy interval from −18.0 to −17.0 eV are essentially constructed from Ge–S covalent bonding interaction with more contributions from sulfur atoms, and those at even lower energies (about −21 eV) are basically of S 3*s* character and were not shown in the figure. It is clear that the Fermi energy is at the top of the valence band, and there is a gap of about 4.0 eV between the filled valence and the empty conduction bands. Therefore, Cu_4GeS_4 is expected to be a semiconducting or insulating type material, in accordance with the resistivity measurements.

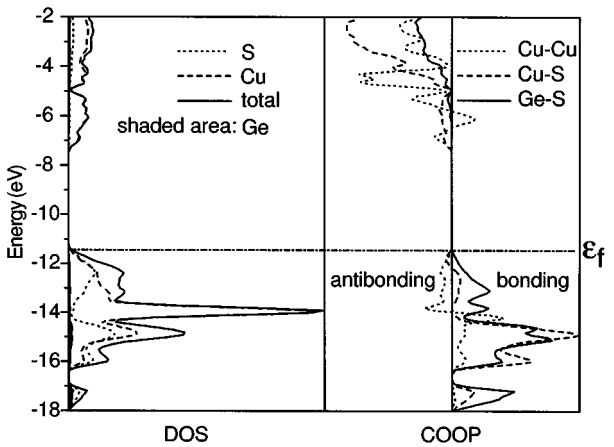

FIG. 5. DOS and COOP curves for Cu_4GeS_4.

The crystal orbital overlap population (COOP) curves in Fig. 5 indicate that Ge–S bonding is optimized, i.e., all of the bonding region is occupied and the antibonding region empty. The germanium–sulfur interactions are indeed quite strong, with the large overlap populations of 0.599–0.650. For the Cu–S bond, the strongly bonding peaks are situated in the lower energy region of the displayed window, while only a weak antibonding peak is observed near the Fermi level. This is due to mixing of the Cu 4*s* and 4*p* orbitals, which enter in a bonding way toward S 3*p* orbitals, thus weakening the Cu 3*d*–S 3*p* antibonding interactions. The calculated Cu–S overlap populations (o.p.) range from 0.107 to 0.475, depending on the distances (2.236(7)–2.634(8) Å), and these values are very comparable to those reported in $BaCu_4S_3$ (o.p. 0.07–0.426 for Cu–S distances of 2.237–2.701 Å) (41). The COOP plot indicates that both Cu–Cu bonding and antibonding 3*d* states are occupied, and the antibonding states are slightly weaker than the corresponding bonding ones owing to the second-order mixing of the Cu 4*s* and 4*p* orbitals into 3*d* orbitals. As a consequence, the integrated COOP gives the small positive values of 0.026, 0.025, and 0.011 for three typical Cu...Cu contacts of 2.665(7), 2.704(5), and 2.812(6) Å, respectively. From these small positive numbers, we cannot conclude that the metal–metal bonds are formed among the closed-shell Cu^+, because at a computational level, net attractive Cu(I)–Cu(I) interactions require the introduction of configuration interaction into Hartree-Fock solutions. It has been shown that interactions between two closed-shell Au^+ (d^{10}) species are repulsive at the Hartree–Fock level (42). Recent density functional calculations on $Cu_2(hpp)_2$ ($hpp^- = C_7N_3H_{12}$ = 1,3,4,6,7,8-hexahydro-2H-pyrimido [1,2-a]pyrimidinate) and $Cu_3[(p\text{-tol})N_5(p\text{-tol})]_3$ (p-tol = $CH_3C_6H_4$ = p-tolyl), which have even shorter Cu...Cu distances of 2.453(1) and 2.353(2) Å, respectively, showed that the close approach of the copper atoms is predictable without involving any significant amount of covalent bonding (43). Therefore, the Cu...Cu distances in Cu_4GeS_4 may be due to the packing necessities and may unnecessarily imply the metal–metal bonding. In addition, the computed overlap population values for three different short S...S contacts (3.582(9), 3.584(7) and 3.591(8) Å) are all slightly negative (−0.020, −0.019, and −0.019, respectively), indicating that there is no significant sulfur–sulfur bonding, in agreement with the van der Waals radii values.

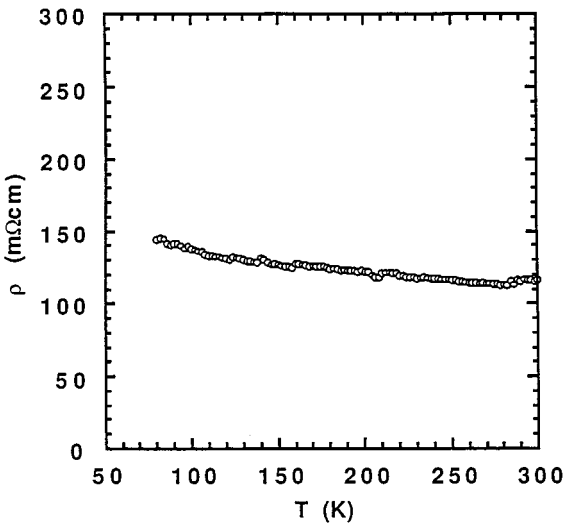

FIG. 6. Electrical resistivity of Cu_4GeS_4 as a function of temperature.

Figure 6 gives a plot of the resistivity ρ vs T for Cu_4GeS_4. Resistivity changed from 115 to 145 m$\Omega \cdot$cm in the temperature range of 300 to 78 K. No phase transition was observed. The electrical property indicates that Cu_4GeS_4 is a semiconducting material. The curvature shows an extrinsic semiconducting behavior with an activation energy of approximately 0.0023 eV at temperatures between 77.8 and 300 K. This result is consistent with the fact that Cu_4GeS_4 is a normal valence compound.

ACKNOWLEDGMENTS

X.-A. C. thanks JST for a STA fellowship. The authors thank Mr. K. Kosuda for carrying out the EPMA analyses.

REFERENCES

1. X. -a. Chen, H. Wada, A. Sato, and M. Mieno, *J. Solid State Chem.* **139,** 144 (1998).
2. X.-a. Chen, H. Wada, and A. Sato, *Mater. Res. Bull.* **34,** No. 2 (1999).
3. N. Wang, *Neues Jahrb. Mineral. Abh.* **159,** 137 (1988).
4. L. M. de Chalbaud, G. D. de Delgado, J. M. Delgado, A. E. Mora, and V. Sagredo, *Mater. Res. Bull.* **32,** 1371 (1997).
5. Gotz, "Institut fur Kristallographie der Aachen, West Germany, ICDD Grant-in-Aid." 1988.
6. N. Rysanek, P. Laruelle, and A. Katty, *Acta Crystallogr. Sect. B* **32,** 692 (1976).
7. M. Levalois and G. Allais, *Acta Crystallogr. Sect. B* **37,** 1816 (1981).
8. N. Wang, *Neues Jahrb. Mineral. Abh.* **126,** 141 (1976).
9. N. Wang and W. Viaene, *Neues Jahrb. Mineral. Monatsh.* 442 (1974).
10. M.-H. Whangbo and R. Hoffmann, *J. Am. Chem. Soc.* **100,** 6093 (1978).
11. M. Brändle and G. Calzaferri, *Helv. Chim. Acta* **76,** 2350 (1993).
12. J. Llanos, P. Valenzuela, C. Mujica, and A. Buljan, *J. Solid State Chem.* **122,** 31 (1996).
13. D. M. Proserpio, G. Artioli, S. Mulley, G. Chacon, and C. Zheng, *Chem. Mater.* **9,** 1463 (1997).
14. J. H. Ammeter, H.-B. Bürgi, J. C. Thibeault, and R. Hoffmann, *J. Am. Chem. Soc.* **100,** 3686 (1978).
15. R. Ramirez and M. C. Böhm, *Int. J. Quantum Chem.* **34,** 571 (1988).
16. M. J. Buerger, *Z. Kristallogr.* **95,** 83 (1936).
17. A. Yamamoto, *Acta Crystallogr. Sect. A* **48,** 476 (1992).
18. B. A. Frenz and Associates, "SDP for Windows Reference Manual, Inc." College Station, TX, 1995.
19. A. Altomare, G. Cascarano, C. Giacovazzo, and A. Guagliardi, *J. Appl. Crystallogr.* **26,** 343 (1993).
20. G. M. Sheldrick, "SHELXL97, a Program for the Refinement of Crystal Structures." University of Göttingen, Germany, 1997.
21. G. B. Jameson, *Acta Crystallogr. Sect. A* **38,** 817 (1982).
22. R. Herbst-Irmer and G. M. Sheldrick, *Acta Crystallogr. Sect B* **54,** 443 (1998).
23. Y. Le Page, *J. Appl. Crystallogr.* **21,** 983 (1988).
24. H. T. Jr. Evans, *Z. Kristallogr.* **150,** 299 (1979).
25. G. Savelsberg and H. Schäfer, *Mater. Res. Bull.* **16,** 1291 (1981).
26. F. Q. Huang, W. Choe, S. Lee, and J. S. Chu, *Chem. Mater.* **10,** 1320 (1998).
27. P. Pyykkö, *Chem. Rev.* **97,** 597 (1997).
28. P. Wu and J. A. Ibers, *J. Solid State Chem.* **107,** 347 (1993).
29. K. O. Klepp and D. Gurtner, *J. Alloys Compd.* **243,** 19 (1996).
30. K. Klepp and K. Yvon, *Acta Crystallogr. Sect. B* **36,** 2389 (1980).
31. M. Ohmasa, M. Suzuki and Y. Takéuchi, *Mineral. J.* **8,** 311 (1977).
32. E. Durand, G. Ouvrard, M. Evain, and R. Brec, *Inorg. Chem.* **29,** 4916 (1990).
33. S. Lee, P. Colombet, G. Ouvrard, and R. Brec, *Inorg. Chem.* **27,** 1291 (1988).
34. F. Boucher, M. Evain, and R. Brec, *J. Alloys Compound* **215,** 63 (1994).
35. J. K. Burdett and O. Eisenstein, *Inorg. Chem.* **31,** 1758 (1992).
36. S. Jaulmes, J. Rivet, and P. Laruelle, *Acta Crystallogr. Sect. B* **33,** 540 (1977).
37. L. Pauling, "The Nature of the Chemical Bond." Cornell University Press, Ithaca, 1960.
38. S. A. Sunshine, D. Kang, and J. A. Ibers, *J. Am. Chem. Soc.* **109,** 6202 (1987).
39. I. D. Brown and D. Altermatt, *Acta Crystallogr. Sect. B* **41,** 244 (1985).
40. T. Balic Zunic and I. Vickovic, *J. Appl. Crystallogr.* **29,** 305 (1996).
41. A. Ouammou, M. Mouallem-Bahout, O. Peña, J.-F. Halet, J.-Y. Saillard, and C. Carel, *J. Solid State Chem.* **117,** 73 (1995).
42. P. Pyykkö, J. Li, and N. Runeberg, *Chem. Phys. Lett.* **218,** 133 (1994).
43. F. A. Cotton, X. Feng, and D. J. Timmons, *Inorg. Chem.* **37,** 4066 (1998).